

## Central Lancashire Online Knowledge (CLoK)

Title	Optimization of sustainable concrete incorporating coarse recycled aggregate using a customized single-factor response surface methodology (CSFRSM) approach
Type	Article
URL	<a href="https://clock.uclan.ac.uk/id/eprint/54762/">https://clock.uclan.ac.uk/id/eprint/54762/</a>
DOI	<a href="https://doi.org/10.1007/s44290-025-00195-y">https://doi.org/10.1007/s44290-025-00195-y</a>
Date	2025
Citation	Almaawali, Said, Aldahdooh, Majed, Alnaamani, Sultan A. M., Ibrahim, Nabil T. and Ng, Choon Aun (2025) Optimization of sustainable concrete incorporating coarse recycled aggregate using a customized single-factor response surface methodology (CSFRSM) approach. <i>Discover Civil Engineering</i> , 2 (1).
Creators	Almaawali, Said, Aldahdooh, Majed, Alnaamani, Sultan A. M., Ibrahim, Nabil T. and Ng, Choon Aun

It is advisable to refer to the publisher's version if you intend to cite from the work.  
<https://doi.org/10.1007/s44290-025-00195-y>

For information about Research at UCLan please go to <http://www.uclan.ac.uk/research/>

All outputs in CLoK are protected by Intellectual Property Rights law, including Copyright law. Copyright, IPR and Moral Rights for the works on this site are retained by the individual authors and/or other copyright owners. Terms and conditions for use of this material are defined in the <http://clock.uclan.ac.uk/policies/>

## Research

# Optimization of sustainable concrete incorporating coarse recycled aggregate using a customized single-factor response surface methodology (CSFRSM) approach

Said Almaawali<sup>1</sup> · Majed A. A. Aldahdooh<sup>2</sup> · Sultan A. M. Alnaamani<sup>3</sup> · Nabil T. Ibrahim<sup>1</sup> · Choon Aun Ng<sup>4</sup>

Received: 1 October 2024 / Accepted: 11 February 2025

Published online: 25 February 2025

© The Author(s) 2025 [OPEN](#)

## Abstract

This study systematically optimizes the coarse recycled aggregate (RA) content in concrete using a customized Single-Factor Response Surface Methodology (CSFRSM). It focuses exclusively on coarse recycled aggregate content as the sole variable to comprehensively evaluate its effects on compressive strength, flexural strength, splitting tensile strength, and workability. A Python-based correlation analysis was integrated to reveal interdependencies among concrete properties and enhance the optimization process. The results demonstrate that increasing RA content from 0 to 50% reduces compressive strength (41.35–28.41 MPa), flexural strength (5.26–4.10 MPa), and splitting tensile strength (3.58–3.36 MPa). The optimal mix was achieved at 27.5% RA replacement, yielding a slump value of 26.90 mm, flexural strength of 4.73 MPa, splitting tensile strength of 3.51 MPa, and compressive strengths of 25.85 MPa at 7 days and 35.10 MPa at 28 days. The findings highlight that CSFRSM provides a robust framework for optimizing concrete properties, supporting the advancement of sustainable construction practices.

**Keywords** Customized RSM · Single-factor optimization · Python-based correlation analysis · Construction wastes · Demolition wastes

## 1 Introduction

The construction industry is one of the largest consumers of natural resources, with aggregate demand estimated at 2.7 billion tons annually in the EU, 900 million tons in the USA, and 700 million tons in Brazil [1, 2]. Construction and demolition waste (CDW), a by-product of this demand, accounts for approximately 36% of global waste production [3]. Improper management and disposal of CDW poses significant environmental challenges, including landscape degradation, environmental contamination, and associated health risks [4, 5]. Recycling CDW into recycled aggregates (RA) offers a sustainable alternative that simultaneously addresses waste management and resource scarcity challenges [6]. However, several limitations hinder its widespread adoption in concrete applications, particularly in structural settings. These include the variability in RA properties, its porous nature, and the presence of adhered mortar [7, 8].

Concrete made with RA, referred to as recycled aggregate concrete (RAC), typically exhibits lower mechanical performance compared to natural aggregate concrete (NAC). Studies have reported compressive strength reductions of up

---

✉ Majed A. A. Aldahdooh, majidaladahdooh@icem.edu.om; maldahdooh@uclan.ac.uk | <sup>1</sup>Department of Civil and Environmental Engineering, University of Nizwa, Nizwa, Oman. <sup>2</sup>Department of Facilities and Construction Project Management, International College of Engineering and Management, University of Central Lancashire (UK), P.C. 111, Muscat, Oman. <sup>3</sup>Department of Civil Engineering, Middle East College, Muscat, Rusayl, Oman. <sup>4</sup>Faculty of Science, Universiti Tunku Abdul Rahman, Kampar, Perak, Malaysia.



to 20% at full RA replacement levels, accompanied by decreased tensile strength, modulus of elasticity, and workability [3, 9, 10]. These reductions are primarily attributed to the weaker interfacial transition zones (ITZs) in RA, which result in higher water absorption and poor bonding properties [7, 11]. Furthermore, the variability in RA properties due to differences in source material and processing methods exacerbates these challenges, leading to inconsistent mechanical behavior [12, 13]. Consequently, many global standards restrict RA replacement levels to approximately 30% in structural concrete applications [3].

To overcome these limitations, researchers have explored various optimization methods to improve performance of RAC. Traditional trial-and-error approaches, though common, are often time-consuming, resource-intensive, and inconsistent, making them impractical for systematic optimization [10, 14]. Advanced computational methods such as artificial neural networks (ANNs) and convolutional neural networks (CNNs), have demonstrated notable predictive accuracy for RAC properties. For example, Joseph, Pachiappan [15] and Chiranjeevi, Kumar [16] employed machine learning (ML) models to predict compressive strength and durability metrics with high precision. However, these methods require extensive datasets, substantial computational resources, and specialized expertise, limiting their practical scalability [17, 18].

An alternative and widely used approach is Response Surface Methodology (RSM), which provides a statistically robust framework for optimizing the properties and performance of concrete. RSM enables the modeling of both individual and interactive effects of variables while minimizing the number of experimental runs. For example, Aldahdooh et al. [19–24] employed RSM to optimize binder content in ultra-high-performance fiber-reinforced cementitious composite (UHPRCC), demonstrating its adaptability for retrofitting damaged structures. Similarly, Aldahdooh, Jamrah [25] optimized the impact of two types of plastic waste on the properties of normal concrete using RSM.

Notable applications of RSM in optimizing RAC properties include studies by Habibi, Ramezaniapour [26] and Rezaei, Memarzadeh [27], which focused on nano-silica content in RAC, yielding improvements in compressive strength and durability. Studies such as Zamir Hashmi, Khan [28] and Agrawal, Waghe [29] utilized RSM to evaluate hybrid concrete mixes with steel fibers, nylon granules, and RA, achieving significant improvements in resistance to aggressive environments. Additionally, Habibi, Ramezaniapour [26] and Gopalakrishna and Dinakar [30] combined silica fume (SF) and ground granulated blast furnace slag (GGBFS) with RA, enhancing both mechanical strength and chloride resistance in RAC. While these studies underscore RSM's versatility in multi-factor optimization, they often obscure the direct effects of RA content as a single variable. This gap, as highlighted in the summarized literature review (Table 1), necessitates a more focused investigation into RA's isolated effects on concrete properties.

Despite these advancements, a significant gap exists in the optimization of RA content in RAC as a single-factor variable. Most existing studies prioritize multi-factor combinations, such as RA with supplementary cementitious materials (SCMs) or fibers, leaving the specific influence of RA content underexplored [3, 26, 29]. Furthermore, while machine learning techniques offer superior predictive capabilities, their practical implementation is often constrained by high resource demands and computational complexity [17, 18]. Additionally, few studies have integrated RSM with advanced analytical tools, such as Python-based correlation analysis, to provide deeper insights into the interactions between RA levels and concrete properties [13, 31], as summarized in Table 1.

This study employs a customized single-factor Response Surface Methodology (CSFRSM) to optimize coarse recycled aggregate (RA) replacement levels in recycled aggregate concrete (RAC). It evaluates the effects of RA on compressive strength, tensile strength, flexural strength, and workability. A Python-based correlation analysis uncovers relationships between RA levels and concrete properties, enhancing optimization. The study develops predictive models, analyzes property interdependencies, and proposes a framework for designing sustainable RAC.

## 2 Research significances

This study is pivotal in promoting sustainable construction practices by addressing the challenges of incorporating RA into concrete. It provides a systematic methodology using a CSFRSM to optimize RA content while evaluating its effects on key properties such as mechanical strengths and workability. The integration of Python-based correlation analysis provides enhanced insights into property interdependencies, facilitating the development of sustainable RAC. By improving the practical utilization of CDW, this research contributes to mitigating environmental impacts, conserving natural resources, and fostering the global adoption of sustainable concrete solutions.

Table 1 Summary of Previous Studies on RAC

Study	Purpose	Aim	Methods Used in Design	Factors	Responses	Major Findings	Remaining Gaps
Rezaei, Memarzadeh [27]	Investigate the mechanical and durability properties of RAC incorporating nano-silica	Optimize nano-silica and RAC levels for improved strength and durability	RSM and Gene Expression Programming (GEP)	Nano-silica content, RAC replacement	Compressive strength, durability indicators	Nano-silica improved strength and durability; optimum nano-silica = 4.5%, RAC = 26%	Limited to specific mix designs and environmental conditions
Habibi, Ramezani-pour [26]	Optimize mix design of concrete with RCA, SF, and GGBFS to balance environmental and durability goals	Develop predictive models for compressive strength and chloride migration	RSM with Central Composite Design (CCD), Life Cycle Assessment (LCA)	RAC content, SF content, GGBFS content	Compressive strength, chloride migration, GWP, service life	SF offsets RCA's strength reduction; GGBFS reduced GWP by 36%. Service life significantly extended	Limited assessment of durability beyond chloride migration; findings specific to mix proportions
Lovato, Possan [10]	Model mechanical properties and durability of RAC with coarse and fine recycled aggregates	Evaluate combined effects of RCA replacement, w/c ratio, and mix design	RSM and non-linear regression with ANOVA	RAC %, FRA %, w/c ratio, aggregate/cement ratio	Compressive strength, tensile strength, elasticity, carbonation depth	Higher RAC and FRA content reduced performance; optimal RAC = 50%, FRA = 50%, w/c ≤ 0.6 for satisfactory results	Limited durability factors evaluated; requires environmental adjustments for scalability
Hammoudi, Mousaceb [32]	Compare ANN and RSM in predicting compressive strength of RAC concrete	Evaluate the precision of RSM vs. ANN for compressive strength prediction at different ages	RSM with CCD and ANN models	RAC %, cement content, slump	Compressive strength (7, 28, 56 days)	ANN achieved higher precision (R <sup>2</sup> = 99.8% vs. 98.7% for RSM); RCA reduced strength due to weak ITZ	Focused only on compressive strength without assessing durability or scalability for other mix designs
Farah Aziera Jamaludin, Loong Jie [33]	Evaluate fresh and mechanical properties of concrete with recycled fine aggregate (RFA) as partial sand replacement	Examine RFA effects on workability, compressive strength, and water absorption	Experimental analysis with 5 mixtures (0%, 10%, 20%, 30%, 40% RFA)	RFA percentage (0–40%)	Slump, compressive strength, water absorption	Optimal RFA content (20%) improved strength, and 40% RFA yielded water absorption < 10%, indicating good quality concrete	Limited evaluation of durability and no predictive modeling
Ahmed, Ali [34]	Investigate polypropylene fiber (PPF) and silica fume effects on recycled aggregate concrete (RAC)	Optimize mechanical properties with RSM	Experimental analysis with RSM optimization	PPF (0–0.9%), SF (0–5%), RAC content (0–100%)	Compressive strength, tensile strength, elasticity	SF and PPF improved RAC performance; optimum PPF was 0.6%	Limited to mechanical properties; durability aspects not covered
Zhang, Feng [35]	Optimize mix design of recycled aggregate pervious concrete	Develop practical mix design with Box-Behnken Design (BBD) and simplex centroid design	Response Surface Methodology (RSM)	Paste properties, aggregate gradation, void content	Compressive strength, porosity, permeability	Optimized mix improved porosity while maintaining adequate strength	No long-term durability evaluation; focus on limited porosity parameters

Table 1 (continued)

Study	Purpose	Aim	Methods Used in Design	Factors	Responses	Major Findings	Remaining Gaps
Aghajanzadeh, Ramezaniapour [13]	Optimize alkali-activated slag concrete with RCA, RFA, and silica fume (SF)	Evaluate mechanical, durability, environmental, and economic factors using RSM	Quadratic RSM modeling with multi-objective optimization	RCA (0–100%), RFA (0–100%), SF (0–20%)	Compressive strength, chloride penetration, CO <sub>2</sub> emission, cost	Optimal mix achieved environmental benefits with minimal strength trade-offs	Limited exploration of alkali-activated concrete's long-term durability
Sun, Fan [36]	Optimize shear properties of RAC with hybrid fibers and nano-SiO <sub>2</sub> (NS)	Develop hybrid system for shear strength optimization	Double shear testing and RSM for multivariate regression	Basalt fiber (0.1–0.7%), PPF (0.1–0.3%), NS (0–3.5%)	Shear strength, toughness, strain, fracture energy	NS-BF-PPF system significantly enhanced shear performance; optimal NS was 3.5%	Limited durability evaluation; results focused on shear properties only
Gopalakrishna and Dinakar [30]	Optimize fly ash-based geopolymer concrete with 100% recycled aggregates (RA)	Develop a novel mix design for geopolymer concrete using RSM and evaluate marine applications	RSM for mix optimization; SEM and XRD for microstructural analysis	Fly ash content, sodium hydroxide concentration, RA ratio	Compressive strength, chloride resistance	Optimal fly ash (35 MPa) and chloride resistance; suitable for marine structures	Limited durability testing beyond chloride ingress; lacks long-term environmental exposure validation
Francioso, Moro [31]	Assess thermal conductivity of mortar with recycled aggregates (RAC) under varying conditions	Evaluate RCA's effect on thermal conductivity with moisture variations	Experimental analysis combined with RSM for modeling	RCA replacement level, saturation degree, ambient temperature	Thermal conductivity, compressive strength, porosity	RAC reduced thermal conductivity but increased moisture sensitivity; models achieved < 5% error	No exploration of real-world building scenarios or insulation performance under dynamic conditions
Zhao, Liu [17]	Review machine learning models for predicting properties of recycled aggregate concrete (RAC)	Compare machine learning models (e.g., ANN, SVM) for predicting workability, strength, and durability	Literature review and statistical comparison	Input variables for ML models: RA content, W/C ratio, curing conditions	Mechanical properties, durability metrics	ML models (especially ANN) provided superior accuracy for nonlinear RAC performance prediction	Lack of real-world validation and limited understanding of hyper-parameter tuning in complex datasets
Ji, Wang [18]	Predict properties of RAC using machine learning (ML) and optimize mix design	Evaluate ML's ability to predict RAC properties with brick and natural aggregates (BNA)	BP neural network, GA-BP, and CNN models compared	Brick aggregate content, W/C ratio, crushing value, SSD, porosity	Compressive strength, durability indices	CNN achieved highest prediction accuracy (R <sup>2</sup> = 0.969); demonstrated intelligent RAC design potential	Limited scalability to diverse mix designs or long-term applications
Agrawal, Waghe [29]	Explore eco-friendly concrete with recycled coarse aggregates (RAC) and rubber particles (RP)	Optimize mechanical and durability properties of RAC-RP concrete using RSM	Experimental analysis with RSM optimization	RCA (0–100%), RP (0–20%)	Compressive strength, durability metrics	Optimal mix (60% RCA, 10% RP) achieved strength comparable to control concrete; enhanced sustainability	Variability in RAC and RP quality; requires improved processing techniques

**Table 1** (continued)

Study	Purpose	Aim	Methods Used in Design	Factors	Responses	Major Findings	Remaining Gaps
Li, Cai [14]	Optimize pervious concrete with recycled aggregates for urban drainage applications	Evaluate mechanical and permeability properties using RSM and numerical modeling	Laboratory experiments with RSM regression modeling	Aggregate size, W/C ratio, target porosity	Compressive strength, permeability coefficient	Optimal design enhanced permeability while maintaining adequate strength; high model accuracy (<5% error)	Focused only on RAP; lacks broader assessment of urban sustainability impacts

### 3 Materials and methods

#### 3.1 Materials

The materials used in this study included Ordinary Portland Cement (OPC) and three types of aggregates: fine aggregates (FA), normal crushed coarse aggregates (NCA), and coarse RA. OPC-52.5N, Type I with a specific gravity of 3.15 and a fineness of 328 m<sup>2</sup>/kg, conforming to BS EN 197-1:11 [37] and ASTM C 150/150 M [38] standards, was utilized in this study. The physical and chemical properties of OPC are provided in Table 2. FA had a maximum particle size of 4.75 mm, a specific gravity of 2.61, and 13.2% material passing through the 75-micron sieve, determined as per BS 812-103.1:85 [39]. Both NCA and RA had a maximum particle size of 20 mm, with specific gravities of 2.74 and 2.61, respectively. The physical and chemical properties of these aggregates are summarized in Table 3.

RA used in this study were produced from CDW collected from the Al-Masnaah and Barka, Oman. The production process involved crushing CDW into smaller fragments, sieving to achieve the desired particle size, and washing to remove impurities and lightweight materials, ensuring clean and well-graded aggregates suitable for concrete production (Fig. 1). To address RA's higher water absorption capacity, pre-saturation was performed, ensuring consistent water-to-cement (w/c) ratios during mixing.

The Los Angeles abrasion value of RA was 30%, compared to 15% for NCA, as per ASTM C131/C131M [40]. RA's water absorption was 4.9%, significantly higher than 0.3% for NCA, tested in accordance with ASTM C127-24: 15 [41].

Key aggregate properties, such as elongation and flakiness indices, were measured as 21% and 11% for RA, and 19% and 3% for NCA, respectively, tested according to BS 812-105.2:90 [42] and BS EN 933-3:12 [43]. The presence of clay lumps and friable particles was recorded at 0.08% for RA and 0.06% for NCA, in compliance with [44]. The percentage of material passing the 75-micron sieve was 1.1% for RA and 0.1% for NCA, tested per ASTM C117-17 [45], while FA was evaluated following BS 812-103.1:85 [39].

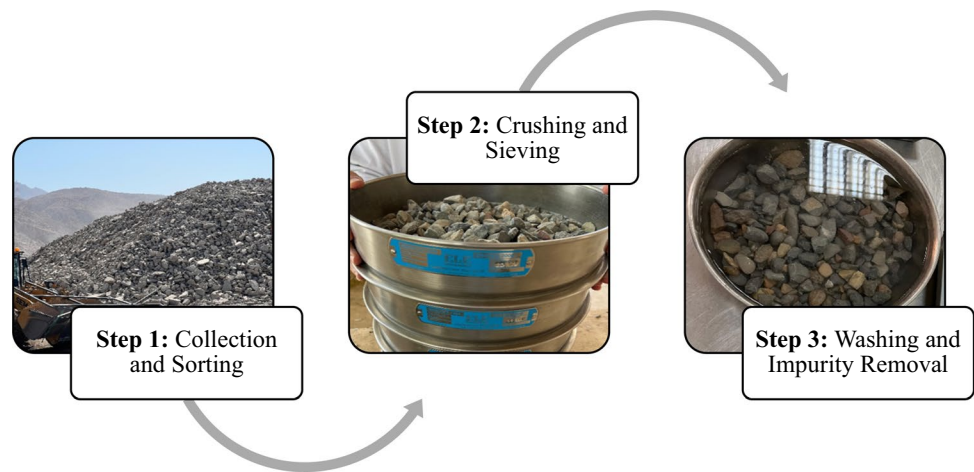
The particle size distribution of RA, NCA, and FA was determined through sieve analysis, with the grading curves presented in Fig. 2. All aggregates complied with the limits specified in BS 882, confirming their suitability for concrete

**Table 2** Physical and Chemical Properties of OPC

Category	Property	Test Result
Physical Test	Specific Surface (m <sup>2</sup> /kg)	334
	Setting Time (Initial, Minutes)	195
	Setting Time (Final, Minutes)	195
	Soundness (Le Chatelier Expansion, mm)	1.0
	Compressive Strength (2 Days, N/mm <sup>2</sup> )	26.4
	Compressive Strength (7 Days, N/mm <sup>2</sup> )	45.5
	Compressive Strength (28 Days, N/mm <sup>2</sup> )	57.5
Chemical Test	Silica (SiO <sub>2</sub> ) %	20.52
	Insoluble Residue (IR) %	0.35
	Alumina (Al <sub>2</sub> O <sub>3</sub> ) %	4.53
	Ferric Oxide (Fe <sub>2</sub> O <sub>3</sub> ) %	3.86
	Lime (CaO) %	63.36
	Magnesia (MgO) %	1.52
	Sulphur Trioxide (SO <sub>3</sub> ) %	2.28
	Loss on Ignition (LOI) %	2.28
	Chloride (Cl <sup>-</sup> ) %	0.02
	Alkalis (Na <sub>2</sub> O + 0.658 K <sub>2</sub> O) %	0.60
	Tricalcium Silicate (C <sub>3</sub> S) %	58.16
	Dicalcium Silicate (C <sub>2</sub> S) %	14.95
	Tricalcium Aluminate (C <sub>3</sub> A) %	5.57
Lime Saturation Factor (LSF)	93.93	
Alumina Modulus (AM)	1.17	

**Table 3** Physical and Chemical Properties of Aggregates

Property	RA	NCA	Standard Used
Specific Gravity	2.61	2.74	ASTM C142/C142M: 17 [44]
Maximum Particle Size (mm)	20	20	ASTM C142/C142M: 17 [44]
Clay Lumps & Friable Particles (%)	0.08	0.06	ASTM C142/C142M: 17 [44]
Material Passing 75 Micron Sieve (%)	1.1	0.1	ASTM C117-17 [45]
Elongation Index (%)	21	19	BS 812-105.2:90 [42]
Soundness (Weight Loss, % over 5 cycles)	NA	2.0	C88/C88M-18 [48]
Water Absorption (%)	4.9	0.3	ASTM C127-24: 15 [41]
Flakiness Index (%)	11	3	BS 812-105.2:90 [42] (RA), BS EN 933-3:12 [43] (NCA)
Los Angeles Abrasion Value (%)	30	15	ASTM C131/C131M [40]
Voided Shell Content (%)	Nil	Nil	BS 812-106:1985 [49]
Ten Percent Fines Value (kN)	140	NA	BS 812-111:90 [50]
Chemical Analysis			
Acid Soluble Chloride Content (Cl <sup>-</sup> ) %	<0.01	0.01	BSI—BS 812-117: 88 [46]
Acid Soluble Sulphate Content (SO <sub>3</sub> ) %	0.05	0.07	BS 812-118:88 [47]
Gypsum Content %	<0.02	<0.02	V.S.Bhatt [51]
Aggregate Crushing Value %	26	NA	BS 812-110:1990 [52]
Aggregate Impact Value %	28	NA	BS 812-112:90 [53]
Weighted Average Percent Loss (%)	8	NA	C88/C88M-18 [48]

**Fig. 1** Steps in the Preparation of Coarse RA

production. RA also met chemical quality requirements, including acid-soluble chloride content (<0.01%) and acid-soluble sulfate content (0.05%), tested per BSI—BS 812-117: 88 [46] and BS 812-118:88 [47].

Additional mechanical properties of RA include an aggregate crushing value (ACV) of 26% and an aggregate impact value (AIV) of 28%, while NCA was not tested for these parameters. The soundness test showed a weight loss of 2% over 5 cycles for NCA, in accordance with C88/C88M-18 [48]. RA's performance in these tests, along with compliance with grading and chemical standards, highlights its suitability for sustainable concrete applications.

### 3.2 Mix design using RSM and correlation analysis

In this study, the control mixture, RA0 (C35-grade), was designed using the DOE method in accordance with BS EN 206-1:2000 [54] standards, with a water-cement ratio (W/C) of 0.57 and a fine aggregate-cement ratio (FA/C) of 1.62. To evaluate the effects of recycled aggregate (RA) on concrete properties, including compressive strength, flexural strength, splitting tensile strength, and workability, a series of mixtures were developed by replacing natural coarse

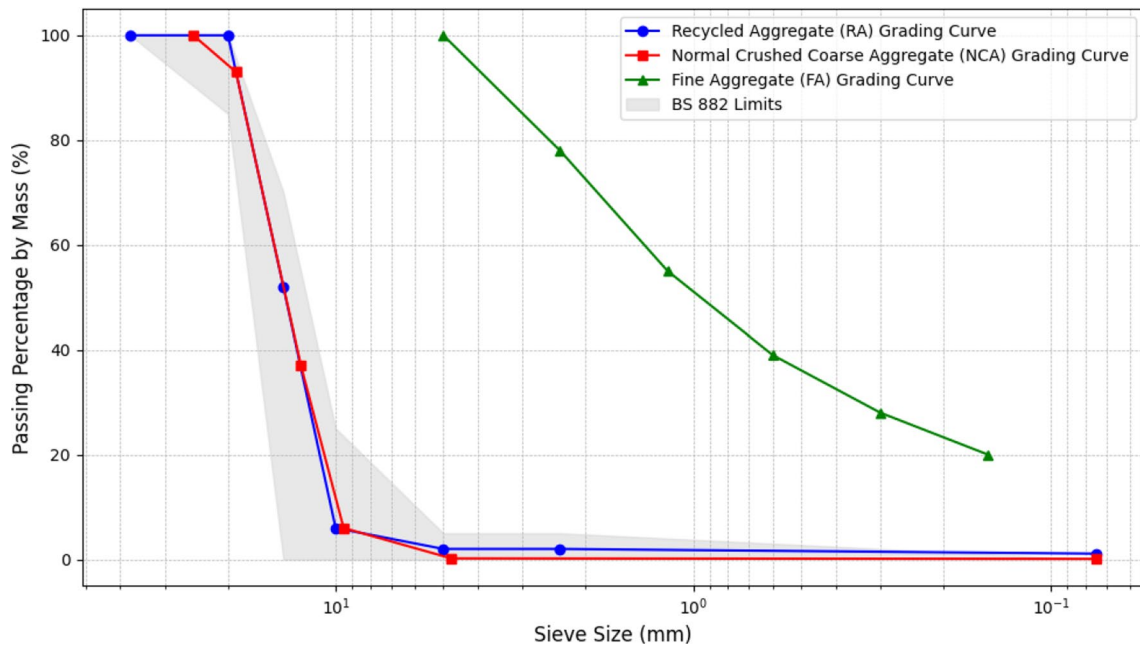


Fig. 2 Grading Curves for RA, NCA and FA aggregates

aggregate (NCA) with RA at levels of 10%, 20%, 30%, 40%, and 50%. These mixtures were denoted as RA10, RA20, RA30, RA40, and RA50, respectively, as outlined in Table 4.

To optimize the performance of these mixtures, a CSFRSM, with a Central Composite Design (CCD), was employed. This approach allowed for an efficient analysis of the effects of the single factor ([NCA-RA]%) on multiple responses: splitting tensile strength ( $Y_1$ ), compressive strength at 7 days ( $Y_2$ ), compressive strength at 28 days ( $Y_3$ ), workability ( $Y_4$ ), and flexural strength ( $Y_5$ ). Using the CSFRSM feature of Design-Expert® 6.0.7 software, 18 experimental runs were generated to evaluate the responses systematically. The quadratic model used for analysis is expressed as:

$$Y = \beta_0 + \sum_{i=1}^k \beta_i X_i + \sum_{i=1}^k \beta_{ii} X_i^2 + \sum_{i < j}^k \sum_{j=1}^k \beta_{ij} X_i X_j + e_i \tag{1}$$

Equation 3 represents the matrix notation of the model:

$$Y = X\beta \pm \epsilon \tag{2}$$

Table 4 Concrete Mix Proportions and Design

Run	Mixture	[NCA-RA] %	W/C	C	Coarse aggregate		
					FA: C	NCA:C	RA:C
1-3	RA0	0	0.57	1	1.62	3.05	0.00
4-6	RA10	10	0.57	1	1.62	2.74	0.30
7-9	RA20	20	0.57	1	1.62	2.44	0.61
10-12	RA30	30	0.57	1	1.62	2.13	0.91
13-15	RA40	40	0.57	1	1.62	1.83	1.22
15-18	RA50	50	0.57	1	1.62	1.52	1.52

[RA0] refers to the control mixture of normal concrete, [NCA-RA]% refers to the replacement level of NCA with RA; [W/C] refers to the water: cement ratio; [FA:C] refers to the fine aggregates: cement ratio; [NCA:C] refers to the normal crushed coarse aggregate: cement ratio; [RA:C] refers to the recycled aggregates: cement ratio

where,  $Y$  is a matrix of predicted responses ( $[Y_1, Y_2]$ ),  $X$  is the matrix of coded values ( $[NCA-RA]\%$ ),  $\beta$  is the matrix of regression coefficients, and  $\epsilon$  is the matrix of random errors. This model enabled the identification of optimal RA replacement levels while minimizing the number of experimental runs required.

### 3.2.1 Analysis and optimization process

ANOVA was employed to analyze the interactions between factors and responses. Statistical significances were assessed using  $R^2$ , P-value, and  $t$ -tests. Diagnostic plots to evaluate model adequacy. This research aims to maximize the RA content in concrete while maintaining optimal workability and mechanical properties. Therefore, optimization constraints, including specific target ranges for factors and responses, were set as detailed in Table 5. Furthermore, a ramp function graph was utilized in this study to identify the ideal region for all responses, contributing to improvements in concrete properties.

### 3.2.2 Correlation analysis

In this study, Python was employed to determine the Pearson and Spearman correlation coefficients to assess the relationships among the following factors:  $[NCA-RA]\%$ , compressive strength after 7 days, compressive strength after 28 days, workability, and flexural strength after 28 days. Using the *pandas* and *numpy* libraries, a correlation matrix was constructed, and *seaborn* was utilized to create a heatmap to visualize these connections. This technique provided a thorough understanding of how  $[NCA-RA]\%$  influences the concrete characteristics.

## 3.3 Specimen preparations and experimental testing procedures

### 3.3.1 Specimen preparations

Specimens were prepared in accordance with ASTM C192/C192M-19a [55] to ensure consistency and reliability. OPC, FA, NCA, RA, and water were accurately measured based on the mix proportions provided in Table 4. Prior to mixing, the recycled aggregates (RAs) were pre-saturated to accommodate their higher water absorption capacity. This step ensured the mix water content and water-to-cement (w/c) ratio remained consistent across all mixtures. All dry materials, including aggregates and binders, were mixed for 1.5 min to achieve uniform distribution. Water was then gradually added while mixing continued for an additional 2.5 min. A final mixing interval of 1 min was performed, resulting in a total mixing time of 5 min. The workability of the fresh concrete was evaluated using the slump test in accordance with ASTM: C143/C143M [56]. The concrete was then poured into molds in two layers, compacted using a vibration table as per BS EN 998-2:16 [57], and demolded after 24 h. The specimens were then cured in water at  $27^\circ\text{C} \pm 2^\circ\text{C}$  following BS EN 12390-2:19 [58] and ASTM C511-19 [59] until the designated testing times.

### 3.3.2 Experimental testing

This study examines the impact of using RA as a replacement for NCA on the properties of normal concrete, including workability, compressive strength, splitting tensile strength, and flexural strengths. The slump test was conducted to evaluate the effect of varying RA replacement levels (RA10, RA20, RA30, RA40, and RA50) on the workability of concrete mixtures, according to BS EN 12390-3:19 [60]. To assess the mechanical properties, three cubic samples (each  $100\text{ mm} \times 100\text{ mm} \times 100\text{ mm}$ ) from each mixture (refer to Table 4) underwent testing with a loading rate of  $0.30\text{ MPa/s}$ , to

**Table 5** Constraints of Optimization for RA Concrete

Name	Goal	Lower Limit	Upper Limit
x: $[NCA-RA]\%$	is in range	25.00	50.00
Splitting Tensile	is in range	3.34	3.58
Compressive Strength @ 7 days	is in range	22.49	30.51
Compressive Strength @ 28 days	is in range	35.00	41.74
Workability	is in range	24.10	29.30
Flexural Strength	is in range	4.08	5.29

examine the effect of RA on the concrete's compressive strength at age of 7 and 28 days, according to BS EN 12390–3:19 [60].

For flexural strength evaluation, three beam specimens (150 mm × 150 mm × 600 mm) per mixture were subjected to testing under a loading rate of 0.06 N/(mm<sup>2</sup>·s) (or 450 N/s) at 28 days, in compliance with BS 1881–118:83 [61]. Flexural strength values were calculated using Eq. (3). For the splitting tensile strength, three cylindrical specimens (150 mm in diameter and 300 mm in height) were subjected to testing at 28 days under a steady loading rate of 0.015 MPa/s until failure, in accordance with BS EN 12390–6:09 [62]. The splitting tensile strength values were calculated using Eq. (4).

$$\text{Flexural Strength} = \frac{P \times l}{bh^2} \quad (3)$$

Where,  $P$  is the maximum load applied (N),  $l$  is the span length (mm),  $b$  is the width of specimen (mm), and  $h$  is the depth of specimen (mm).

$$\text{Indirect Tensile Strength (MPa)} = \frac{2 \times P}{\pi \times H \times D} \quad (4)$$

Where,  $P$  is the maximum load applied (N);  $H$  is the specimen height (mm);  $D$  is the sample diameter (mm).

## 4 Results and discussions

This section interprets the findings of slump, compressive strength, flexural strength, and splitting tensile strength tests. It is also discussing the results from correlation analysis, mathematical modeling, statistical analysis and the optimization process.

### 4.1 Impact of RA on concrete properties

Figures 1 and 2 illustrate the impact of varying recycled aggregate (RA) replacement levels ([NCA-RA]%) on the properties of concrete and their corresponding relative indices, while Fig. 4 explores the correlations between concrete properties and these replacement levels. The results demonstrate a notable reduction in concrete properties as the [NCA-RA]% levels increase.

At both 7 and 28 days, the compressive strength shows a consistent decline with increasing [NCA-RA]% levels, as depicted in Fig. 3. At 28 days, compressive strength decreases from 41.35 MPa (100%) for the control mixture (RA0) to 28.41 MPa (68.70%) for R50, while at 7 days, it reduces from 30.25 MPa (100%) for RA0 to 22.60 MPa (74.71%) for R50. Moderate RA levels (e.g., R20) retain compressive strength more effectively, with values of 37.80 MPa at 28 days (91.40%) and 27.98 MPa at 7 days (92.49%), as illustrated in Fig. 4. This trend is supported by Lovato, Possan [10], Zhao, Liu [17], Habibi, Ramezani pour [26], and Gopalakrishna and Dinakar [30], which attribute the reduction in compressive strength

Fig. 3 Impact of RA on Concrete Properties

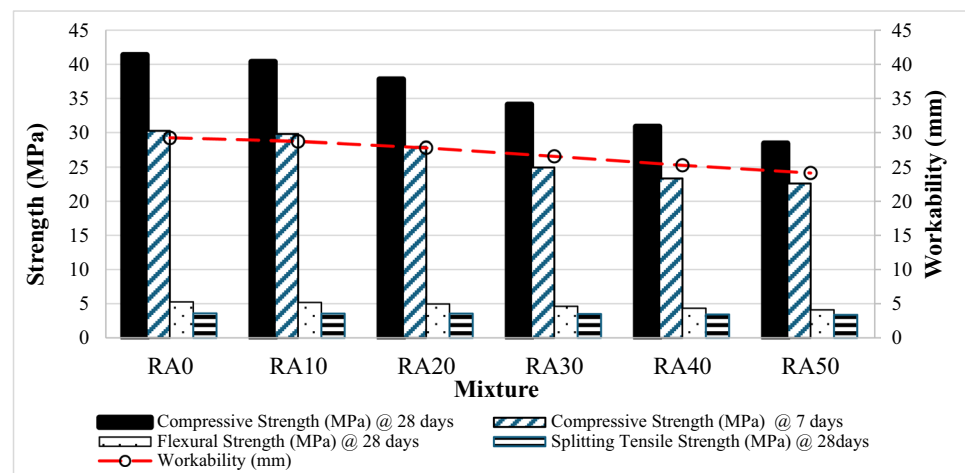
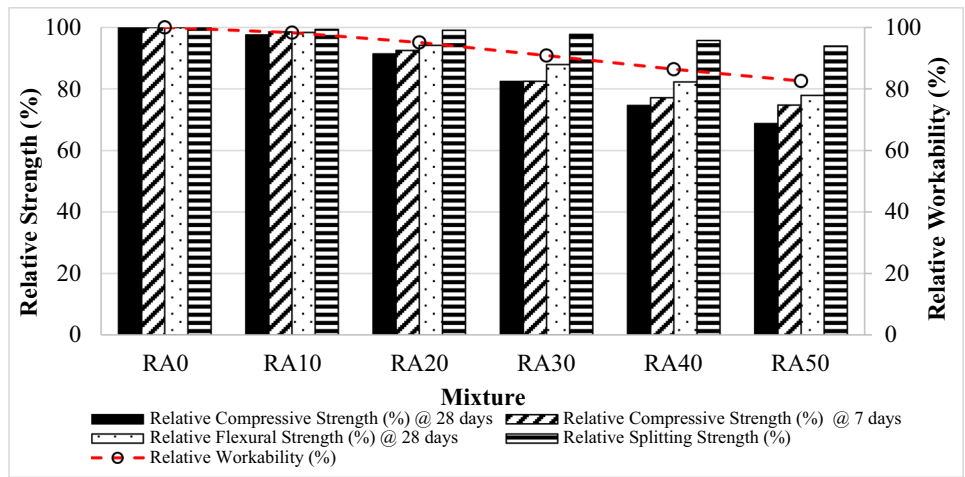


**Fig. 4** Relative Index of Concrete Properties for Each Mixture



to weaker interfacial transition zones (ITZ) and the higher porosity of recycled aggregates. Agrawal, Waghe [29] observed that moderate RA levels (20–30%) retained over 90% of the control compressive strength, consistent with the performance of R20 in this study. The correlation analysis in Fig. 5 demonstrates a near-perfect negative correlation ( $r = -0.99$ ) between [NCA-RA]% and compressive strength, consistent with findings from previous studies Ji, Wang [18], Hammoudi, Moussaceb [32] and Francioso, Moro [31], which highlight the weakening effects of RA on ITZ and overall matrix bonding.

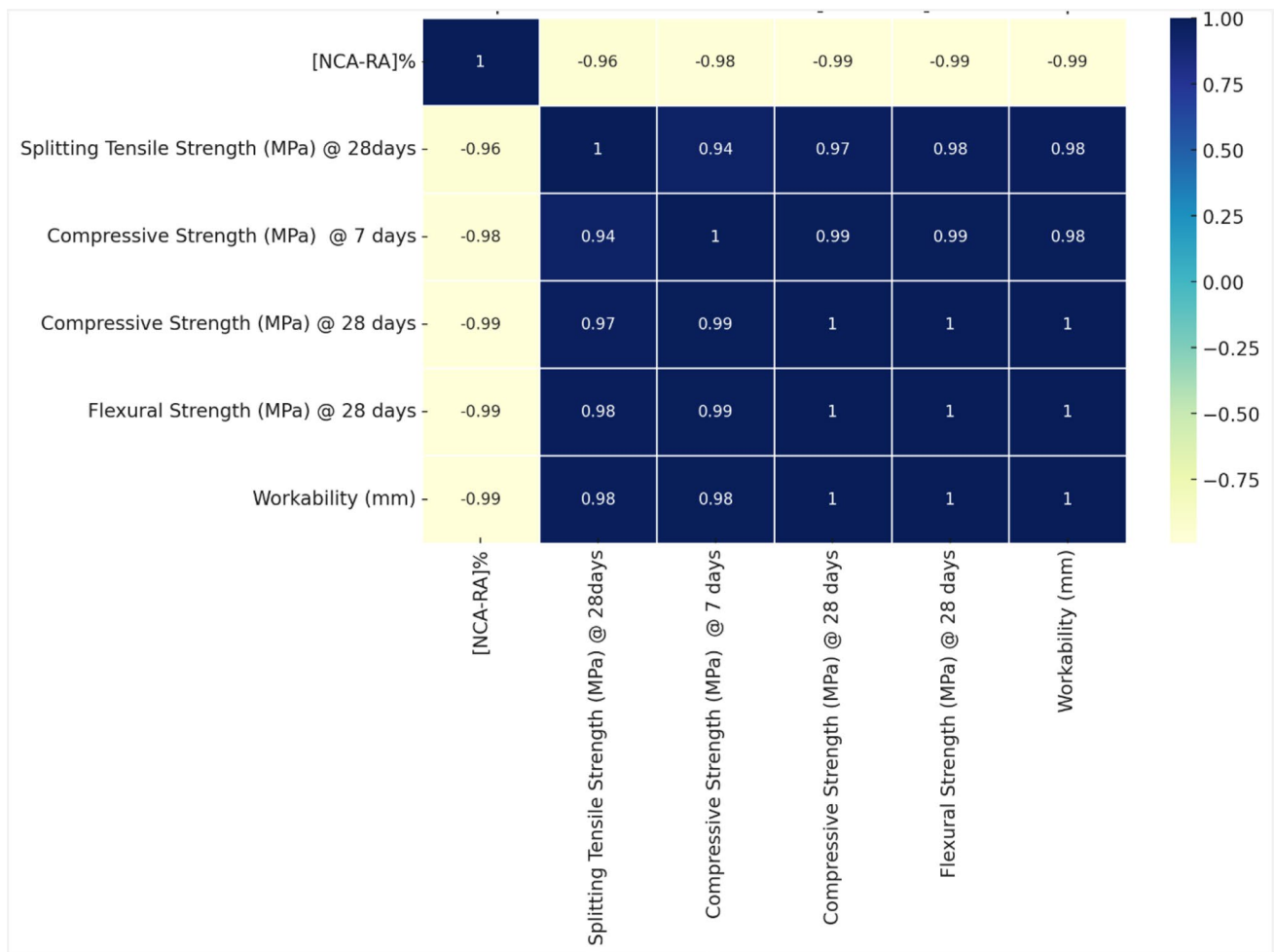


**Fig. 5** Correlation Analysis of Concrete Properties and [NCA-RA]%

Additionally, Aghajanzadeh, Ramezaniapour [13] and Habibi, Ramezaniapour [26] emphasized that RA levels up to 30% sustain sufficient compressive strength for practical applications, validating the balance achieved at moderate replacement levels in this study. These results confirm that while higher RA levels significantly reduce compressive strength, moderate RA levels (20–30%) maintain acceptable performance for structural applications.

The splitting tensile strength at 28 days exhibits a consistent decline with increasing RA levels, as shown in Fig. 3. The strength decreases from 3.58 MPa (100%) for the control mixture (RA0) to 3.36 MPa (93.93%) for R50. Despite this reduction, moderate RA levels (e.g., R20) retain tensile strength close to the control, with a value of 3.55 MPa (99.10% relative strength), as shown in Fig. 4. This trend is supported by Lovato, Possan [10], Zhao, Liu [17], Habibi, Ramezaniapour [26], and Gopalakrishna and Dinakar [30], of which observed declines in tensile strength with increasing RA content, attributing the reduction to weaker bonding at the interfacial transition zones (ITZ) and the higher porosity of RA compared to natural aggregates. Furthermore, Study Agrawal, Waghe [29] found that moderate RA levels (20–30%) retain splitting tensile strength close to the control, aligning with the observed 99.10% relative strength for R20 in this study. The correlation analysis in Fig. 5 confirms a strong negative correlation ( $r = -0.96$ ) between [NCA-RA]% and tensile strength, emphasizing the sensitivity of this property to RA levels. These findings validate that while higher RA levels reduce tensile strength, moderate replacement levels (20–30%) sustain performance close to the control, making them a practical choice for structural applications.

The flexural strength decreases consistently with increasing [NCA-RA]% levels, as depicted in Fig. 3. At 28 days, the flexural strength reduces from 5.26 MPa (100%) for RA0 to 4.10 MPa (77.86%) for R50. Moderate replacement levels, such as R20, retain flexural strength reasonably well, achieving 4.96 MPa (94.18% relative strength), as shown in Fig. 4. This trend aligns with the findings of Lovato, Possan [10] and Zhao, Liu [17], which reported similar reductions in flexural strength due to the weaker mechanical properties and porous nature of RA. Agrawal, Waghe [29] further support these findings, showing that moderate RA levels (20–30%) retain over 90% of flexural strength, consistent with the observed performance of R20 in this study. The correlation analysis in Fig. 5 confirms a near-perfect negative correlation ( $r = -0.99$ ) between [NCA-RA]% and flexural strength, emphasizing the sensitivity of this property to RA content. The reduction in flexural strength at higher RA levels is attributed to weaker bonding at the interfacial transition zones (ITZ) and the structural limitations of RA, as observed in previous studies [13, 26, 31]. These findings confirm that while higher RA levels significantly reduce flexural strength, moderate RA replacement levels (20–30%) provide sufficient performance for structural applications.

The workability of the concrete mixtures, measured by slump, decreases significantly with increasing RA levels, as shown in Fig. 3. The slump is reduced from 29.24 mm (100%) for RA0 to 24.14 mm (82.56%) for R50. However, at moderate replacement levels such as R20, workability remains relatively high at 27.81 mm (95.12% relative workability), as shown in Fig. 4. This decline in workability is attributed to the properties of RA, including its higher water absorption (4.9% vs. 0.3% for NCA), rougher surface texture, and greater angularity, as detailed in Table 3. These characteristics increase the water demand of the mix, leading to reduced flowability, aligning with findings from Zhang, Feng [35]. Similarly, Lovato, Possan [10] and Zhao, Liu [17] reported consistent declines in workability with increasing RA content, particularly beyond 30% replacement. The correlation analysis in Fig. 5 confirms a near-perfect negative correlation ( $r = -0.99$ ) between [NCA-RA]% and workability, consistent with Francioso, Moro [31], which identified RA's porous structure and angularity (e.g., elongation index of 21% vs. 19% for NCA and flakiness index of 11% vs. 3% for NCA) as key contributors to reduced slump. Despite these reductions, moderate RA levels (20–30%) ensure acceptable workability, as indicated by the 95.12% relative workability for R20 in this study, supported by Gopalakrishna and Dinakar [30] and Agrawal, Waghe [29]. These results confirm that while higher RA levels reduce workability due to their physical and chemical properties, moderate replacement levels maintain sufficient flowability for practical applications.

The analysis of Figs. (3–5) confirm that increasing RA levels ([NCA-RA]%) negatively impact concrete properties, with strong negative correlations (e.g.,  $r = -0.99$  for compressive and flexural strengths, and workability;  $r = -0.96$  for splitting tensile strength). At 28 days, compressive strength declines from 41.35 MPa (100%) for RA0 to 28.41 MPa (68.70%) for R50, while R20 retains 37.80 MPa (91.40%). Splitting tensile and flexural strengths follow similar trends, with R20 maintaining 99.10% and 94.18% relative strengths, respectively. Workability also decreases, with R20 retaining 95.12%, compared to 82.56% for R50. These results align with Lovato, Possan [10], Zhao, Liu [17], Habibi, Ramezaniapour [26], and Gopalakrishna and Dinakar [30], which attribute performance declines to weaker interfacial zones and higher porosity in recycled aggregates. The strong interdependence among mechanical properties ( $r = 0.94$  to 1.00) observed in Fig. 5 supports studies by Zhang, Feng [35] and Agrawal, Waghe [29], emphasizing that changes in one property influence others. While high RA levels significantly reduce performance, moderate replacements (20–30%) sustain sufficient strength and workability, offering a practical balance for sustainable structural applications.

**Table 6** ANOVA Results and Model Validation

Responses	Model Significance	Significant Model Terms	Adjusted R <sup>2</sup>	Predicted R <sup>2</sup>	Adeq Precision
Splitting Tensile @ 28 days	Significant	$x, x^2$	0.95	0.94	29.01
Compressive Strength @ 7 days	Significant	$x, x^2, x^3$	0.97	0.97	32.20
Compressive Strength @ 28 days	Significant	$x, x^2, x^3$	0.99	0.99	89.55
Workability	Significant	$x, x^2, x^3$	0.99	0.99	197.40
Flexural Strength @ 28 days	Significant	$x, x^2$	0.98	0.98	56.24

[Adeq Precision] refers to the signal-to-noise ratio; [Adjusted R<sup>2</sup>] adjusts the R<sup>2</sup> value for the number of predictors in a regression model; [Predicted R<sup>2</sup>] estimates how well the model predicts new data; [x] refers to the replacement levels [NCA-RA]%

**Table 7** Final Equation in Terms of Actual Factors

Response	Equation
Splitting Tensile Strength @ 28 days	$= 3.575 - 0.00027x - 8.16 \times 10^{-5}x^2$
Compressive Strength @ 7 days	$= 30.251 + 0.0766x - 0.0135x^2 + 0.00018x^3$
Compressive Strength @ 28 days	$= 41.346 + 0.0213x - 0.0132x^2 + 0.00015x^3$
Workability	$= 29.232 - 0.0162x - 0.0035x^2 + 3.56 \times 10^{-5}x^3$
Flexural Strength @ 28 days	$= 5.300 - 0.0156x - 0.00019x^2$

[x] refers to the replacement level of NCA with RA [NCA-RA]%

## 4.2 Mathematical modeling and statistical analysis results

Models of compressive strength, flexural strength, splitting tensile strength, and workability were evaluated using key statistical metrics, including predicted R<sup>2</sup>, adjusted R<sup>2</sup>, and Adeq Precision measures (see Table 6). For the splitting tensile strength model, the predicted R<sup>2</sup> was 0.94, and the adjusted R<sup>2</sup> was 0.95, indicating strong predictive accuracy and model fit. The compressive strength at 7 days demonstrated both a predicted R<sup>2</sup> and an adjusted R<sup>2</sup> of 0.97, reflecting excellent consistency between observed and predicted values. Similarly, the models for compressive strength at 28 days and workability each exhibited both a predicted R<sup>2</sup> and adjusted R<sup>2</sup> of 0.99, emphasizing their exceptional predictive reliability. Finally, the flexural strength model achieved a predicted R<sup>2</sup> and adjusted R<sup>2</sup> of 0.98, further validating its robustness. These findings confirm the reliability and robustness of all evaluated models, establishing their suitability as predictive tools for optimizing the recycled aggregate (RA) content in concrete mixtures.

The equations derived from the evaluated models are outlined in Table 7. These equations establish the relationship between the factors (x) and the responses (concrete properties), providing a valuable tool for predictive analysis and facilitating optimized mix design.

### 4.2.1 Analysis and numerical optimization results

The analysis demonstrates the predictive model's accuracy and reliability in optimizing concrete mixtures. Figure 6 shows a strong alignment between predicted and actual values, with a normal distribution of residuals confirming the model's robustness. Figures 7 and 8 identify the optimal [NCA-RA]% of 27.5%, achieving a splitting tensile strength of 3.51 MPa, compressive strengths of 25.85 MPa (7 days) and 35.10 MPa (28 days), workability of 26.88 mm, and flexural strength of 4.73 MPa. The ramp function graph in Fig. 8 confirms this optimal point with a desirability score of 1.0, showing reduced performance beyond this percentage. These results validate the model's effectiveness in balancing mechanical properties and workability for optimized concrete designs.

Table 8 demonstrates the reliability of the RSM model, showcasing minimal residuals across all responses (ranging from—0.06 to—0.84 MPa for mechanical properties and—0.09 mm for workability). The strong correlation between predicted and experimental values further validates the model's accuracy in optimizing recycled aggregate concrete. Ongoing validation with independent mixes will be included in the revised manuscript to reinforce these findings.

**Fig. 6** Model Analysis for: **a** Splitting Tensile Strength @ 28 days, **b** Compressive Strength @ 7 days, **c** Compressive Strength @ 28 days **d** Workability Flexural Strength @ 28 days

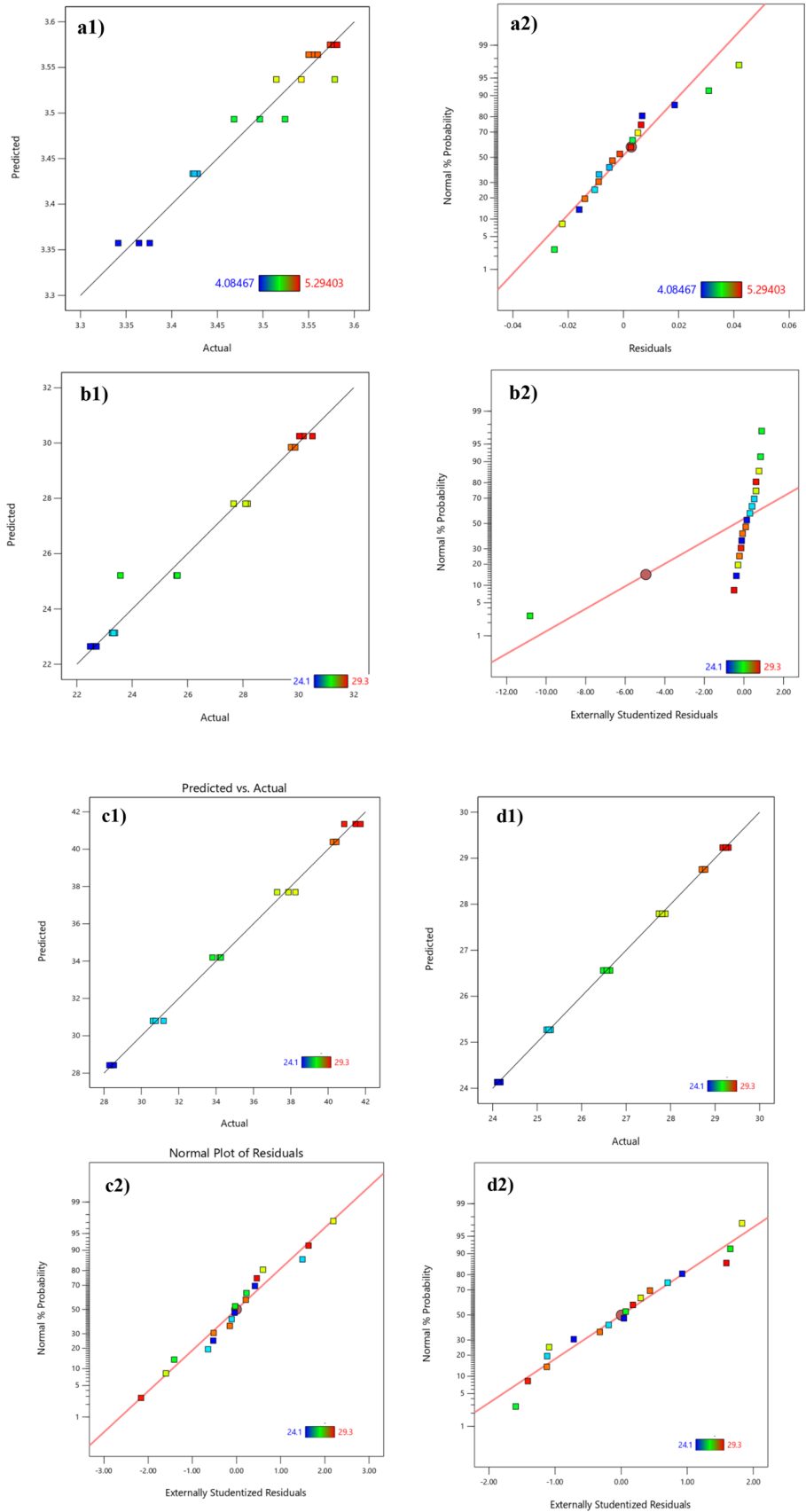


Fig. 6 (continued)

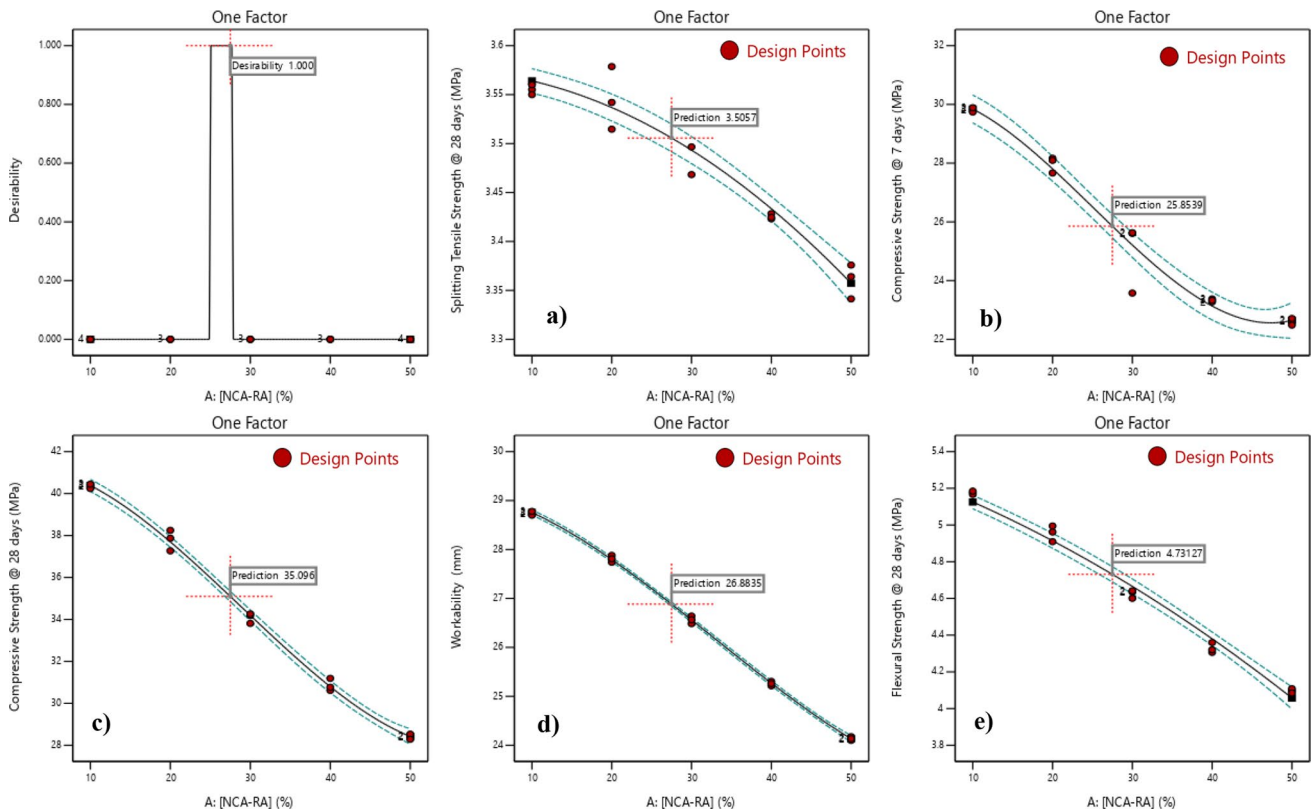
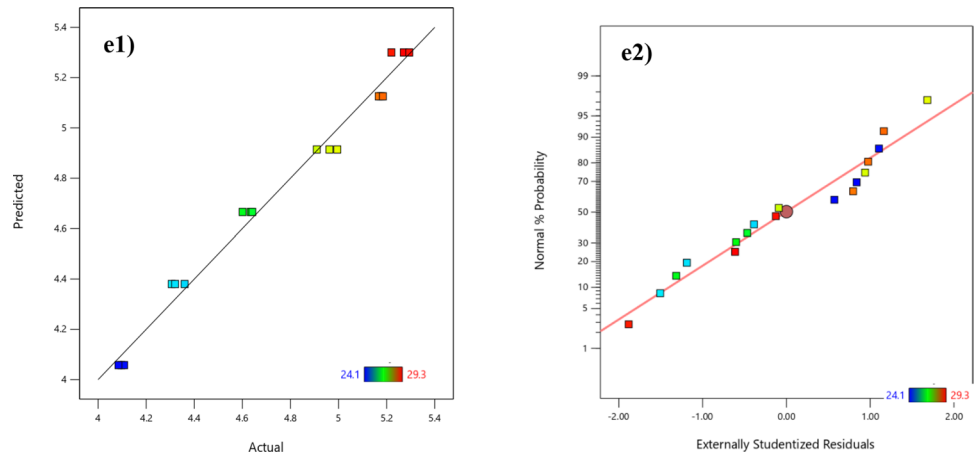


Fig. 7 One Factor Prediction Plot: **a** Splitting Tensile Strength (MPa) @ 28 days model, **b** Compressive Strength (MPa) @ 7 days model, **c** Compressive Strength (MPa) @ 28 days model, **d** Workability (mm) model, and **e** Flexural Strength (MPa) @ 28 days model.

### 5 Conclusion

This study examined the impact of coarse recycled aggregate (RA) on concrete properties and developed predictive models to optimize RA content for sustainable concrete. The key conclusions are summarized as follows:

- Increasing RA replacement levels significantly reduces concrete properties. For instance, at 50% RA (R50), the compressive strength at 28 days decreased to 28.41 MPa (68.70% relative strength), flexural strength reduced to 4.10 MPa (77.86% relative strength), and workability declined to 24.14 mm (82.56% relative workability).

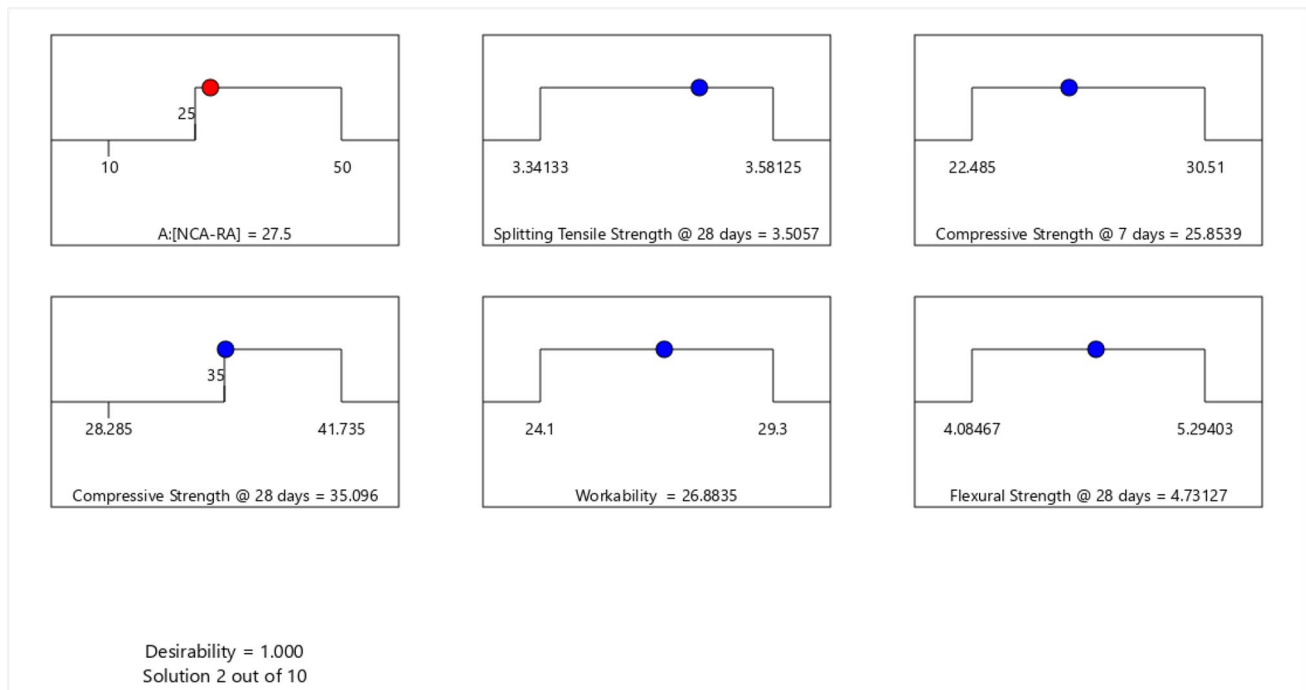


Fig. 8 Ramp Function Graph Analysis for Optimal [NCA-RA] %

Table 8 Comparison of Predicted and Experimental Results for the Optimal Concrete Mixture

Response	Predicted value	Actual Value	Residual
Splitting Tensile Strength @ 28 days (MPa)	3.56	3.44	- 0.12
Compressive Strength @ 7 days (MPa)	25.85	25.01	- 0.84
Compressive Strength @ 28 days (MPa)	35.10	34.50	- 0.6
Workability (mm)	26.88	26.79	- 0.09
Flexural Strength @ 28 days (MPa)	4.73	4.67	- 0.06

- Concrete maintains performance comparable to the control mixture (RA0) at moderate RA levels (20%-30%). The R20 mixture achieved a compressive strength of 37.80 MPa (91.40% relative strength), splitting tensile strength of 3.55 MPa (99.10% relative strength), flexural strength of 4.96 MPa (94.18% relative strength), and workability of 27.81 mm (95.12% relative workability) at 28 days.
- Strong negative correlations ( $r = -0.97$  to  $-1.00$ ) between [NCA-RA]% and concrete properties indicate that higher RA content adversely affects performance. Conversely, positive correlations ( $r = 0.96$  to  $1.00$ ) among concrete properties suggest that improvements in one property often enhance others.
- The predictive models developed for forecasting concrete properties demonstrated exceptional accuracy. Both Predicted  $R^2$  and Adjusted  $R^2$  values exceeded 0.97, confirming the reliability of these models.
- The optimal [NCA-RA]% was identified as 27.5%, achieving a perfect desirability score of 1.0. At this level, the concrete properties included a compressive strength of 35.10 MPa at 28 days, splitting tensile strength of 3.51 MPa, flexural strength of 4.73 MPa, and workability of 26.88 mm, striking an ideal balance for practical applications.

While this study provides significant insights into optimizing coarse recycled aggregate (RA) content using a customized single-factor response surface methodology (CSFRSM) model, some aspects could be further explored. The variability in RA properties due to differences in source and processing methods may influence results under varying conditions. Expanding future research to include a broader range of RA sources could enhance the applicability of these findings. Additionally, while this research focuses on short-term mechanical properties to establish foundational insights, investigating long-term durability aspects, such as resistance to freeze–thaw cycles and chloride penetration, would further validate RA-concrete’s suitability for structural applications.

**Acknowledgements** The authors express their gratitude to BE'AH-Oman Company for providing construction and demolition waste samples. Additional thanks are extended to the Ministry of Higher Education, Research, and Innovation (MoHERI), Oman, for their financial support under grant reference MoHERI/BFP/ICEM/2022.

Permissions for third-party materials: All of the material is owned by the authors and/or no permissions are required.

**Author contributions** S.A.: Supervision, Resources, Conceptualization, Project Administration, Writing – Review & Editing. M.A.: Formal Analysis, Visualization, Validation, Software, Methodology, Writing – Review & Editing. S.A. and N.T.: Investigation, Writing – Original Draft. C.N.: Writing – Review & Editing.

**Funding** This research was supported by the Ministry of Higher Education, Research, and Innovation (MoHERI), Oman, under grant reference MoHERI/BFP/ICEM/2022. The funding body had no role in the design of the study, collection, analysis, interpretation of data, or in writing the manuscript.

**Data availability** All data generated or analyzed during this study are included in this published article. Additional raw data supporting the findings of this study are available from the corresponding author upon reasonable request.

## Declarations

**Ethics approval and consent to participate** This research did not involve human or animal subjects, their data, or biological materials. Ethics, Consent to Participate, and Consent to Publish declarations: Not applicable.

**Consent to publication** The results/data/figures in this manuscript have not been published elsewhere, nor are they under consideration (from you or one of your Contributing Authors) by another publisher.

**Competing interests** I declare that the authors have no competing interests as defined by Discover, or other interests that might be perceived to influence the results and/or discussion reported in this paper.

**Open Access** This article is licensed under a Creative Commons Attribution-NonCommercial-NoDerivatives 4.0 International License, which permits any non-commercial use, sharing, distribution and reproduction in any medium or format, as long as you give appropriate credit to the original author(s) and the source, provide a link to the Creative Commons licence, and indicate if you modified the licensed material. You do not have permission under this licence to share adapted material derived from this article or parts of it. The images or other third party material in this article are included in the article's Creative Commons licence, unless indicated otherwise in a credit line to the material. If material is not included in the article's Creative Commons licence and your intended use is not permitted by statutory regulation or exceeds the permitted use, you will need to obtain permission directly from the copyright holder. To view a copy of this licence, visit <http://creativecommons.org/licenses/by-nc-nd/4.0/>.

## References

1. Silva R, De Brito J, Dhir R. Properties and composition of recycled aggregates from construction and demolition waste suitable for concrete production. *Construct Build Mater*. 2014. <https://doi.org/10.1016/j.conbuildmat.2014.04.117>.
2. de Andrade Salgado, F. and F. de Andrade Silva, Recycled aggregates from construction and demolition waste towards an application on structural concrete: a review. *J Build Eng*. 2022. <https://doi.org/10.1016/j.jobe.2022.104452>
3. Etxeberria M, et al. Influence of amount of recycled coarse aggregates and production process on properties of recycled aggregate concrete. *Cement Concret Res*. 2007. <https://doi.org/10.1016/j.cemconres.2007.02.002>.
4. Poon CS, et al. Influence of moisture states of natural and recycled aggregates on the slump and compressive strength of concrete. *Cement Concret Res*. 2004. [https://doi.org/10.1016/S0008-8846\(03\)00186-8](https://doi.org/10.1016/S0008-8846(03)00186-8).
5. Ithraa Oman, Briefings from oman waste management, In the public authority for investment promotion and export development. 2017: Oman.
6. ABRELPE, E.A.J.S.P.G., Panorama dos resíduos sólidos no Brasil. 2012
7. Kou S-C, Poon C-S. Long-term mechanical and durability properties of recycled aggregate concrete prepared with the incorporation of fly ash. *Cement Concret Composit*. 2013. <https://doi.org/10.7764/rdlc.22.1.178>.
8. de Oliveira MB, Vazquez E. The influence of retained moisture in aggregates from recycling on the properties of new hardened concrete. *Waste Manag*. 1996. [https://doi.org/10.1016/S0956-053X\(96\)00033-5](https://doi.org/10.1016/S0956-053X(96)00033-5).
9. Bravo M, et al. Mechanical performance of concrete made with aggregates from construction and demolition waste recycling plants. *J Clean Product*. 2015. <https://doi.org/10.1016/j.jclepro.2015.03.012>.
10. Lovato PS, et al. Modeling of mechanical properties and durability of recycled aggregate concretes. *Construct Build Mater*. 2012. <https://doi.org/10.1016/j.conbuildmat.2011.06.043>.
11. Habibi A, et al. RSM-based evaluation of mechanical and durability properties of recycled aggregate concrete containing GGBFS and silica fume. *Construct Build Mater*. 2021. <https://doi.org/10.1016/j.conbuildmat.2020.121431>.

12. Tam VW, Gao X, Tam CM. Microstructural analysis of recycled aggregate concrete produced from two-stage mixing approach. *Cement Concret Res*. 2005. <https://doi.org/10.1016/j.cemconres.2004.10.025>.
13. Aghajanzadeh I, et al. Mixture optimization of alkali activated slag concrete containing recycled concrete aggregates and silica fume using response surface method. *Construct Build Mater*. 2024. <https://doi.org/10.1016/j.conbuildmat.2024.135928>.
14. Li F, et al. Mechanical and permeability analysis and optimization of recycled aggregate pervious concrete based on response surface method. *J Renew Material*. 2023. <https://doi.org/10.32604/jrm.2022.024380>.
15. Joseph HS, et al. Prediction of the mechanical properties of concrete incorporating simultaneous utilization of fine and coarse recycled aggregate. *Revista de la construcción*. 2023. <https://doi.org/10.7764/rdlc.22.1.178>.
16. Chiranjeevi K, et al. Optimisation of recycled concrete aggregates for cement-treated bases by response surface method. *Intern J Pave Eng*. 2023. <https://doi.org/10.1080/10298436.2023.2179051>.
17. Zhao Z, et al. Prediction of properties of recycled aggregate concrete using machine learning models: a critical review. *J Build Eng*. 2024. <https://doi.org/10.1016/j.jobbe.2024.109516>.
18. Ji Y, Wang D, Wang J. Study of recycled concrete properties and prediction using machine learning methods. *J Build Eng*. 2024. <https://doi.org/10.1016/j.jobbe.2024.110067>.
19. Aldahdooh, M., et al., 5 GUSMRC—From concept to structural application. 2017. 7: p. 133
20. Aldahdooh M, Bunnori NM, Johari MM. Influence of palm oil fuel ash on ultimate flexural and uniaxial tensile strength of green ultra-high performance fiber reinforced cementitious composites. *Material Des*. 2014. <https://doi.org/10.1016/j.matdes.2013.08.094>.
21. Aldahdooh MAA. Utilization of by-product materials in ultra high-performance fiber reinforced cementitious composites, in cement based materials. France: IntechOpen; 2018.
22. Aldahdooh MAA, Muhamad Bunnori N, Megat Johari MA. Evaluation of ultra-high-performance-fiber reinforced concrete binder content using the response surface method. *Material Design*. 2013. <https://doi.org/10.1016/j.matdes.2013.06.034>.
23. Aldahdooh MA, et al. Improving damaged reinforced concrete beam failure behavior using externally bonded uhpfrccs system. *Intern J Civil Eng*. 2023. <https://doi.org/10.1007/s40999-022-00734-z>.
24. Aldahdooh MAA, et al. Retrofitting of damaged reinforced concrete beams with a new green cementitious composites material. *Compos Struct*. 2016. <https://doi.org/10.1016/j.compstruct.2016.01.067>.
25. Aldahdooh MAA, et al. Influence of various plastics-waste aggregates on properties of normal concrete. *J Build Eng*. 2018. <https://doi.org/10.1016/j.jobbe.2018.01.014>.
26. Habibi A, et al. RSM-based evaluation of mechanical and durability properties of recycled aggregate concrete containing GGBFS and silica fume. *Construct Build Material*. 2021;270: 121431.
27. Rezaei F, et al. Mechanical features and durability of concrete incorporating recycled coarse aggregate and nano-silica: Experimental study, prediction, and optimization. *J Build Eng*. 2023. <https://doi.org/10.1016/j.jobbe.2023.106715>.
28. Zamir Hashmi SR, et al. Prediction of strength properties of concrete containing waste marble aggregate and stone dust—modeling and optimization using RSM. *Materials*. 2022. <https://doi.org/10.3390/ma15228024>.
29. Agrawal D, et al. Optimization of eco-friendly concrete with recycled coarse aggregates and rubber particles as sustainable industrial byproducts for construction practices. *Heliyon*. 2024. <https://doi.org/10.1016/j.heliyon.2024.e25923>.
30. Gopalakrishna B, Dinakar P. An innovative approach to fly ash-based geopolymer concrete mix design: utilizing 100 % recycled aggregates. *Structures*. 2024. <https://doi.org/10.1016/j.jistruc.2024.106819>.
31. Francioso V, Moro C, Velay-Lizancos M. Effect of recycled concrete aggregate (RCA) on mortar's thermal conductivity susceptibility to variations of moisture content and ambient temperature. *J Build Eng*. 2021. <https://doi.org/10.1016/j.jobbe.2021.103208>.
32. Hammoudi A, et al. Comparison of artificial neural network (ANN) and response surface methodology (RSM) prediction in compressive strength of recycled concrete aggregates. *Construct Build Material*. 2019. <https://doi.org/10.1016/j.conbuildmat.2019.03.119>.
33. Jamaludin FA, et al. Fresh and mechanical properties of concrete containing recycled fine aggregate as partial sand replacement. *Material Today Proceed*. 2023. <https://doi.org/10.1016/j.matpr.2023.06.331>.
34. Ahmed TW, Ali AAM, Zidan RS. Properties of high strength polypropylene fiber concrete containing recycled aggregate. *Constr Build Mater*. 2020. <https://doi.org/10.1016/j.conbuildmat.2020.118010>.
35. Zhang Q, et al. Mix design for recycled aggregate pervious concrete based on response surface methodology. *Constr Build Mater*. 2020. <https://doi.org/10.1016/j.conbuildmat.2020.119776>.
36. Sun D, et al. Experimental study and multi-objective optimization of the shear mechanical properties of recycled aggregate concrete with hybrid fibers and nano SiO<sub>2</sub>. *Constr Build Mater*. 2024. <https://doi.org/10.1016/j.conbuildmat.2024.136463>.
37. BS EN 197-1:11, Cement: Composition, specifications and conformity criteria for common cements. BSI.
38. ASTM: C150/C150M, Standard Specification for Portland Cement. 2009, ASTM International: West Conshohocken, PA 55555, United States.
39. BS 812-103.1:85, Testing aggregates. Method for determination of particle size distribution. BSI.
40. ASTM C131/C131M, Standard test method for resistance to degradation of small-size coarse aggregate by abrasion and impact in the Los Angeles machine. 2006, ASTM International, West Conshohocken, PA.
41. ASTM C127-24: 15, Standard test method for relative density (specific gravity) and absorption of coarse aggregate. ASTM International: West Conshohocken, PA.
42. BS 812-105.2:90, Testing Aggregates—Part 105: methods for determination of particle shape—section 105.2 elongation index of coarse aggregate. . BSI: London.
43. BS EN 933-3:12, Tests for geometrical properties of aggregates. Determination of particle shape. Flakiness index. BSI: London
44. ASTM C142/C142M: 17, Standard test method for clay lumps and friable particles in aggregates. ASTM International: West Conshohocken, PA.
45. ASTM C117-17, Standard Test Method for Materials Finer than 75- $\mu$ m (No. 200) Sieve in Mineral Aggregates by Washing. ASTM International: West Conshohocken, PA.
46. BSI - BS 812-117: 88, Testing aggregates - Part 117: Method for determination of water-soluble chloride salts. BSI London.
47. BS 812-118:88, BS 812-118:1988 Testing Aggregates—Part 118: Methods for determination of sulphate content. BSI: London.

48. C88/C88M-18, A., Standard Test method for soundness of aggregates by use of sodium sulfate or magnesium sulfate. . ASTM International: West Conshohocken, PA.
49. BS 812–106:1985, Testing Aggregates—Part 106: method for determination of shell content in coarse aggregate. . BSI: London.
50. BS 812–111:90, Testing Aggregates—part 111: methods for determination of ten per cent fines value (TFV). BSI: London.
51. V.S.Bhatt, Agriculture Handbook. 2016: US Department of Agriculture.
52. BS 812–110:1990 Testing Aggregates—part 110: methods for determination of aggregate crushing value (ACV). BSI: London.
53. BS 812–112:90, Testing Aggregates—Part 112: Method for determination of aggregate impact value (AIV). . BSI: London.
54. BS EN 206–1:2000, Concrete - Part 1: Specification, performance, production and conformity. 2000, European Standard
55. ASTM C192/C192M-19a, Standard practice for making and curing concrete test specimens in the laboratory. ASTM International: West Conshohocken, PA.
56. ASTM: C143/C143M, Standard test method for slump of hydraulic-cement concrete. 1998, astm international: West Conshohocken, PA 19428–2959, United States.
57. BS EN 998–2:16, Specification for mortar for masonry. Masonry mortar BSI.
58. BS EN 12390–2:19, Testing Hardened Concrete—Part 2: making and curing specimens for strength tests. BSI: London.
59. ASTM C511–19. Standard specification for mixing rooms, moist cabinets, moist rooms, and water storage tanks used in the testing of hydraulic cements and concretes, PA: ASTM International: West Conshohocken.
60. BS EN 12390–3:19, Testing hardened concrete - Compressive strength of test specimens. 2019, BSI.
61. BS 1881–118:83, Testing concrete - Method for determination of flexural strength. BSI.
62. BS EN 12390–6:09, Testing hardened concrete. Tensile splitting strength of test specimens. BSI.

**Publisher's Note** Springer Nature remains neutral with regard to jurisdictional claims in published maps and institutional affiliations.